PRAMANA
— journal of
physics

© Indian Academy of Sciences

Vol. 57, Nos 5 & 6
Nov. & Dec. 2001
pp. 1041–1059

Spinning solitons in cubic-quintic nonlinear media

LUCIAN-CORNEL CRASOVAN[1], BORIS A MALOMED[2] and DUMITRU MIHALACHE[1]
[1]Department of Theoretical Physics, Institute of Atomic Physics, P.O. Box MG-6, Bucharest, Romania
[2]Department of Interdisciplinary Sciences, Faculty of Engineering, Tel Aviv University, Tel Aviv 69978, Israel

Abstract. We review recent theoretical results concerning the existence, stability and unique features of families of bright vortex solitons (doughnuts, or 'spinning' solitons) in both conservative and dissipative cubic-quintic nonlinear media.

Keywords. Optical solitons; spinning solitons; spiral solitons.

PACS Nos 42.65.Tg; 42.81.Dp

1. Introduction

One of the most important achievements in nonlinear science has been the discovery of *solitons*, which are self-localized solutions of certain nonlinear partial differential equations describing the evolution of nonlinear dynamical systems with an infinite number of degrees of freedom [1,2]. The solitons preserve their shape upon interaction and can be viewed as 'nonlinear modes' of the corresponding physical system. They are usually attributed to the so called completely integrable models, which are usually obtained as extreme simplifications of complex physical systems. However, solitons or more properly *solitary waves* in nonintegrable systems (either Hamiltonian or dissipative ones) can also be regarded as nonlinear modes, being qualitatively different from their counterparts in completely integrable systems. Thus, the rather complicated behaviour of the system may be described in terms of just a few degrees of freedom. It is important to notice that in nondissipative Hamiltonian systems, the solitary waves form as a result of a balance between diffraction and/or dispersion and nonlinearity, whereas in dissipative systems, gain and loss must also be balanced. In the former situation, the solitons form continuous families with one (or few) parameter families, whereas in the latter case the additional balance between gain and loss results in a solitary wave solution having the amplitude and width fixed by the parameters of the governing equations, i.e., soliton solutions are isolated ones.

The generic equation which describes dissipative physical systems in a vicinity of a subcritical bifurcation is the complex Ginzburg-Landau (GL) equation, or, in other terms, the nonlinear Schrödinger (NLS) equation perturbed by terms accounting for gain and losses. It exhibits various kind of solutions such as pulselike and shocklike ones, sources, sinks and pulsating (periodic and quasiperiodic) solutions. The GL equation and its different modifications describe various effects in laser physics [3], fluid dynamics [4] and nonlinear optics [5]. The cubic GL equation has been analyzed mainly in the context of plasma physics [6], and its solitary wave solutions are known to be unstable.

Later, the cubic-quintic (CQ) GL equation was put forward, as it admits stable pulselike solutions [7–12]. An interesting generalization of the stable pulselike solution of the CQ GL equation in the two-dimensional (2D) case is the possibility of formation of *spinning* solitons having the shape of a ring vortex (i.e., with a hole in the middle). We will see that, in contrast to a recently found azimuthal instability of spinning doughnut-shaped solitons in the CQ NLS equation, their GL counterparts may be *completely stable*.

On the other hand, a problem of fundamental interest is the possibility of the formation of fully three-dimensional (3D) optical spatiotemporal solitons, also referred to as *light bullets* (LBs). These are non-diffracting and non-dispersing spatially focused short pulses propagating in a bulk medium. LBs have been attracting a growing interest in the last decade, as they are expected to be new fundamental physical objects with a potential for using them in all-optical processing of information. It is well known that stable optical spatiotemporal solitons [13–15] may exist in non-Kerr multidimensional nonlinear optical media. Indeed, while LBs cannot be stable in the Kerr ($\chi^{(3)}$) medium with the simple cubic nonlinearity because of the wave collapse [16], stability can be achieved in media with saturable [17,18], quadratic ($\chi^{(2)}$) [19–21], or CQ [22,23] nonlinearity. A fully localized LB in three dimensions (3D) has not yet been observed, but successful experiments with quasi-two-dimensional (quasi-2D) spatiotemporal solitons in $\chi^{(2)}$ bulk materials, such as $LiIO_3$ and Ba_2BO_4, have been recently reported [24].

In this context, a natural generalization is a spinning LB in the form of a ring vortex or 'doughnut'. In this case, the stability is the issue, as, unlike their $s = 0$ counterparts (s is the spin), the spinning bullets are prone to be unstable against azimuthal perturbations. In 2D models with $\chi^{(2)}$ and saturable nonlinearities, numerical simulations have revealed a strong azimuthal instability [25], which was later observed experimentally in a $\chi^{(2)}$ medium [26]. As a result of this instability, an initial LB with $s = 1$ splits into three (in the $\chi^{(2)}$ medium) or two (in the saturable one) fragments, each being a moving $s = 0$ LB, so that the original 'spin momentum', which must be conserved, is transformed into the orbital momentum of the fragments.

The first accurate study of the spinning LBs in the 3D $\chi^{(2)}$ medium was performed recently [27], demonstrating a similar instability against azimuthal perturbations. Therefore, a challenging problem is to find a physically meaningful model in which spinning LBs would be stable or, at least, whose instability would be weak enough to admit their experimental observation. In this relation, it may be relevant to compare the situation with that for *optical vortices*, i.e., *dark* spinning solitons supported by a finite background. It is well known that, in $\chi^{(2)}$ media, the background is always modulationally unstable [28], hence the optical vortex cannot be stable either. Nevertheless, it was recently possible to experimentally observe this object in a setup designed so that the instability did not have enough room to develop and destroy the vortex [29].

A model which has a chance to feature (quasi) stable spinning LBs is that with the CQ nonlinearity, which postulates a nonlinear correction to the medium's refractive index in the form $\delta n = n_2 I - n_4 I^2$, I being the light intensity. Obviously, this correction can be formally obtained from the expansion of the saturable nonlinearity, with $\delta n = n_2 I \left[1 + \left(n_4/n_2\right) I\right]^{-1}$. However, an important difference is that, while the saturable nonlinearity is always self-focusing, having $\mathrm{d}(\delta n)/\mathrm{d}I > 0$, the CQ nonlinearity changes its character from focusing into defocusing at a critical intensity $I_{\mathrm{cr}} = n_2/(2n_4)$. An experimental measurement of the nonlinear dielectric response in the so-called PTS optical crystal suggests that just the CQ nonlinearity (rather than the saturable one) may adequately model this medium [30].

Direct numerical simulations of the dynamics of 2D solitons with $s = 1$ in the CQ model were first reported in ref. [31] (the stability of 2D solitons with $s = 0$ in the same model was checked by means of direct simulations essentially later [22]). In ref. [31] it has been concluded that the spinning 2D LB is fairly robust, provided that its energy was not too small. It was shown to be robust not only against small perturbations, but also against collisions, which were found to be nearly elastic. Three-dimensional LBs in the CQ model were recently considered by means of the variational approximation in ref. [23], and their full numerical simulations have then demonstrated that the spinning solitons, unlike their $s = 0$ counterparts, are *unstable* [32]. However, a difference from the earlier discovered spinning-LB's instability in the $\chi^{(2)}$ model [27] is that, in the CQ one, the azimuthal instability may be (depending on values of the parameters) much *weaker*, giving a chance to observe spinning LBs in the experiment.

Thus, there appears a natural question, why are the spinning 2D solitons stable in the CQ model (at least for large soliton energies), as it was stated in ref. [31], while in the 3D version of the same model they are definitely unstable [32], although the instability may sometimes be fairly weak? A more accurate direct numerical analysis of the spinning-LB's stability in the CQ model in 2D has been performed recently [33]. It has been found that the spinning LBs turn out to be *always unstable* against azimuthal perturbations (independently, a similar conclusion was made by Neshev [34]). Nevertheless, similar to what was found in 3D, the instability may be growing, depending on the LB's energy, much slower than in the 2D $\chi^{(2)}$ model, and in some cases it is found to be so slow that the spinning soliton becomes virtually stable, from the viewpoint of a possible experiment in a finite-size sample. In particular, this argument may explain an observation of an effectively stable spatial vortex soliton in a non-Kerr 3D optical medium reported in a recent experimental work [35].

In the next section we discuss the properties of both 2D and 3D spinning solitons in conservative cubic-quintic nonlinear media. In §3 we present the unique features of 2D spinning solitons in dissipative cubic-quintic media in comparison with those that exist in the corresponding conservative systems. The conclusions are briefly summarized in the final section.

2. Spinning solitons in dissipativeless cubic-quintic media

A. *Two-dimensional case*

We consider propagation of the electromagnetic field envelope A ($I = |A|^2$) in a CQ isotropic dispersive medium either in a 2D (planar) waveguide, or in a bulk medium in which the field does not depend on one of the transverse coordinates, the latter case corresponding to conditions of the real experiment [24]. An equation governing the evolution of the field is a modified NLS equation,

$$2i\kappa_0 A_z + A_{xx} + \kappa_0 D A_{\tau\tau} + 2\kappa_0^2(n_2/n_0)|A|^2 A - 2\kappa_0^2(n_4/n_0)|A|^4 A = 0, \qquad (1)$$

where $\kappa_0(\omega)$ is the carrier's wave number, which is a function of its frequency ω, $D = -\kappa_0'' > 0$ is the temporal dispersion coefficient which is assumed *anomalous* (solitons cannot exist if the dispersion is normal, with $D < 0$), x and z are the transverse and propagation coordinates, and $\tau \equiv t - \kappa_0' z$ is the so-called reduced time. Rescaling the variables as $u \equiv A\sqrt{n_4/n_2}$, $T \equiv \tau \cdot n_2\sqrt{2\kappa_0/Dn_0n_4}$, $Z \equiv z \cdot \kappa_0 n_2^2/n_0n_4$, and $X \equiv x \cdot \kappa_0 n_2\sqrt{2/n_0n_4}$, we transform eq. (1) into a normalized form,

$$iu_Z + u_{XX} + u_{TT} + |u|^2 u - |u|^4 u = 0. \tag{2}$$

One arrives at exactly the same equation, considering *spatial evolution*, along the z axis, of a stationary field in the bulk medium [31]. In this case, the temporal variable X is replaced by the second transverse coordinate Y. However, the physical interpretation of the solitons is quite different in this case: they should be realized not as 2D or quasi-2D spatiotemporal solitons, but rather as cylindrical beams in the 3D space, which are usually refered to as (2+1)D spatial solitons.

First, we look for stationary solutions to eq. (2) of the form $u = U(r)\exp(is\theta)\exp(i\kappa Z)$, where r and θ are polar coordinates in the (X,T) plane, κ is a wave number shift (relative to the carrier wave), which is also frequently called a propagation constant, and the integer s is the above-mentioned spin. The amplitude U can be taken real, and it obeys an equation

$$U'' + r^{-1}U' - s^2r^{-2}U - \kappa U + U^3 - U^5 = 0. \tag{3}$$

The wave number κ parametrizes a family of stationary solutions. In the 2D and 3D cases (the latter one pertains to 3D spinning LBs, and differs by an extra factor 2 in front of the second term in eq. (3)), the existence regions for LBs are [31,23]: $0 < \kappa < \kappa_{\text{offset}}^{(2\text{D})} \approx 0.18$; $0 < \kappa < \kappa_{\text{offset}}^{(3\text{D})} \approx 0.15$, and in both cases they practically do not depend on the spin [23]. Note that a soliton solution to the 1D version of eq. (2) is known in an exact elementary form, the corresponding exact offset wave number being $3/16 = 0.1875$, so that the above values are quite close to it (see ref. [23] and references therein).

The energy ('number of photons') of LB is

$$E_{2D} = \int_{-\infty}^{\infty}\int_{-\infty}^{\infty} |u(X,T)|^2 \,\mathrm{d}X\,\mathrm{d}T, \tag{4}$$

which is a conserved quantity (a dynamical invariant of eq. (2)). The other obvious dynamical invariants in the 2D case are the Hamiltonian (which is not called 'energy' in this context),

$$H_{2D} = \int_{-\infty}^{\infty}\int_{-\infty}^{\infty} \left[|u_X|^2 + |u_T|^2 - (1/2)|u|^4 + (1/3)|u|^6\right] \mathrm{d}X\,\mathrm{d}T, \tag{5}$$

momentum (equal to zero for the solution considered), and the z-component of the angular momentum,

$$L_{2D} = \int_{-\infty}^{\infty}\int_{-\infty}^{\infty} (\partial\phi/\partial\theta)\,|u|^2 \mathrm{d}X\,\mathrm{d}T, \tag{6}$$

ϕ being the phase of the complex field u. Using eq. (3), one can readily find that $L_{2D} = sE_{2D}$, and

$$H_{2D} = -(2\pi/3)\int_0^\infty rU^6(r)\mathrm{d}r. \tag{7}$$

We have numerically found one-parameter families of the 2D spinning-LB solutions which have the form of a ring vortex with a hole in the center [33]. In accordance with results predicted by means of the semi-analytical variational approximation developed in ref. [31] (see also ref. [23]), the solutions exist provided that their energy exceeds a certain threshold value. As a test for the accuracy of numerical computations, we used an exact relation which can be obtained directly from eq. (3):

$$\kappa E_{2D} = \pi\int_0^\infty rU^4(r)\mathrm{d}r - (2\pi/3)\int_0^\infty rU^6(r)\mathrm{d}r. \tag{8}$$

To quantify the LB solutions, in figure 1 we show the nonlinear wave number κ and the Hamiltonian H_{2D} for the $s=0$, $s=1$, and $s=2$ solitons vs. their energy E_{2D}. In the figure, continuous and dashed lines correspond to branches that prove to be stable and unstable in further simlations. Note that κ monotonously increases with E_{2D}, showing saturation to the above-mentioned limiting value $\kappa_{\text{offset}}^{(2D)}$, at large values of E_{2D}. This dependence was regarded in ref. [31] as an extra evidence in favor of stability of spinning LB for large energies. We also see that the threshold energy for the LB formation dramatically increases with s.

By means of direct simulations of eq. (2), we have found that the spinning LBs are *always* unstable against azimuthal perturbations. Eventually, the instability leads to breakup of the ring vortex into several $s=0$ solitons that fly out in tangential directions. An example for $s=1$ is displayed in figure 2. We have found that the splitting process is *slowed down* with the increase of κ or, accordingly, with the increase of the soliton's energy, which complies with the apparent stability of the high-energy $s=1$ solitons in the 2D CQ model reported in ref. [31].

Thus, spinning LBs with a large energy, having the outer radius much larger than the size of the inner bubble, may turn out to be effectively stable in experiments with finite-size samples. A necessary condition for this is that LB survives over a distance which is several times larger than the soliton period, $Z_0 \equiv \pi/2\kappa$ (this is a characteristic propagation

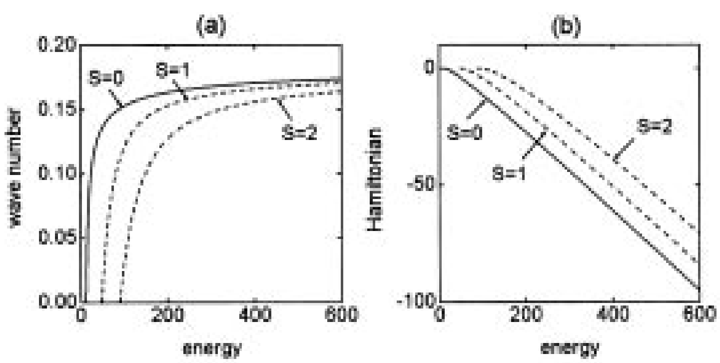

Figure 1. (**a**) The propagation constant κ and (**b**) Hamiltonian H_{2D} of the two-dimensional nonspinning and spinning light bullets vs the energy E_{2D}.

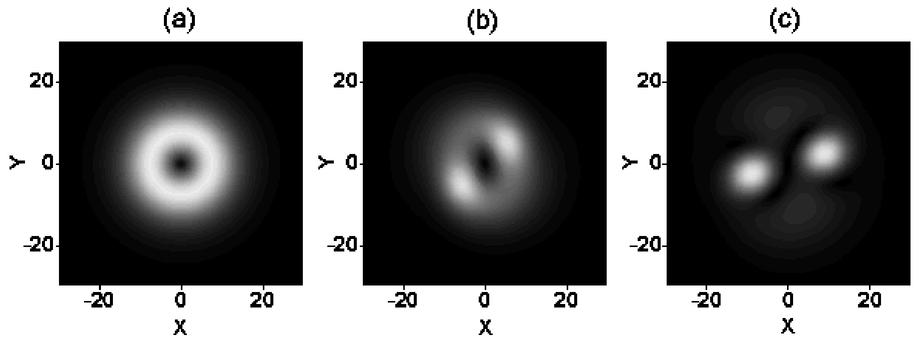

Figure 2. Gray-scale contour plots illustrating the evolution of an unstable two-dimensional spinning light bullet with $s = 1$ and $\kappa = 0.05$: (**a**) $Z = 0$, (**b**) $Z = 310$, and (**c**) $Z = 330$.

length necessary for the formation of the soliton). To estimate whether the propagation distance over which LB survives is large as compared to Z_0, we notice that, in the case $s = 1$ and $\kappa = 0.05$ (figure 2), numerical data show that the splitting actually commences at $Z_{\text{split}} \simeq 300$, while the corresponding soliton's period is $Z_0 \approx 30$. Thus, this vortex ring propagates stably over $\simeq 10$ soliton periods. For a larger value of the propagation constant, $\kappa = 0.14$, hence larger soliton energy, we find $Z_{\text{split}} \simeq 600$ while $Z_0 \approx 10$, so that the LB may be regarded as a *virtually stable* object. We always observed a trend to the stabilization of the spinning LBs with the increase of their energy (i.e., increase of κ). Note that, on the contrary to the situation with the CQ model, the instability of the spinning solitons in the 2D [25] and 3D [27] $\chi^{(2)}$ models, as well as in the 2D saturable one [25], is very strong, so they cannot exist stably in those models even within one soliton's period.

We have also performed simulations for $s = 2$. A general conclusion is that, with the increase of s, the number N of the fragments produced by the eventual breakup of the spinning solitons increases, roughly, as $N = 2s$. Nevertheless, at a fixed value of the spin different numbers of fragments are possible. For instance, N decreases from 4 to 3 with the increase of κ at $s = 2$. This may be construed too as a manifestation of the general trend to stabilize the spinning LB with the increase of its energy. In connection with this, we notice that recently a similar effective stability over large propagation distances was found in simulations of 2D two-component (vector) solitons in a model with a saturable nonlinearity, in which one component carries vorticity [36].

The investigation of the linearized version of eq. (2) provides for the most revealing information for the understanding of the instability of the spinning LBs. The general scheme of this procedure is well known: one seeks for a perturbation eigenmode in the form

$$\delta u = \exp(\gamma_n z + is\theta) \left[\mathscr{U}_+(r) \exp(in\theta) + \mathscr{U}_-(r) \exp(-in\theta)\right] , \tag{9}$$

where s is the spin of the unperturbed solution, and $n > 0$ is an arbitrary integer azimuthal index ('quantum number') of the perturbation; this choice of the perturbation provides for its closedness, i.e., no new angular harmonic will appear in the linearized equations. The instability growth rate γ_n is to be found as an eigenvalue of the linear boundary-value problem for the functions $\mathscr{U}_\pm(r)$:

$$
\begin{aligned}
& i\gamma_n \mathscr{U}_+ + \mathscr{U}_+'' + r^{-1}\mathscr{U}_+' - (s+n)^2 r^{-2}\mathscr{U}_+ \\
& \qquad + \left(2-3U^2\right) U^2 \mathscr{U}_+ + \left(1-2U^2\right) U^2 \mathscr{U}_-^* = 0, \\
& i\gamma_n \mathscr{U}_- + \mathscr{U}_-'' + r^{-1}\mathscr{U}_-' - (s-n)^2 r^{-2}\mathscr{U}_- + \left(2-3U^2\right) U^2 \mathscr{U}_- \\
& \qquad + \left(1-2U^2\right) U^2 \mathscr{U}_+^* = 0,
\end{aligned} \tag{10}
$$

where the asterisk stands for the complex conjugation, $U(r)$ is the unperturbed real solution, and the boundary conditions are that the functions $\mathscr{U}_\pm(r)$ must decay exponentially at $r \to \infty$, and must vanish, respectively, as r^{s+n} and $r^{|s-n|}$ at $r \to 0$.

For the numerical solution of eqs (10) we used a known procedure which is described, e.g., in refs [25,37], and [38]. Skipping further technical details, in figure 3 we show the results for the one-parameter families of the spinning solitons presented in figure 1. In accordance with the direct simulations of eq. (2), the azimuthal number n of the perturbation eigenmode that exhibits the largest growth rate was found to depend on the value of the spin, being $n = 2$ for $s = 1$, and either $n = 3$ or $n = 4$ for $s = 2$. Thus, for example, if the perturbation with the azimuthal number $n = 4$ has the largest growth rate, we may expect that the axial symmetry of the spinning soliton is broken by the perturbation and reduced to the four-fold symmetry, at least at early stages of the propagation.

Summarizing many numerical results, we have concluded that the number N of the emerging fragments, observed in direct numerical simulations of eq. (2), in most cases coincides with the index n of the largest growth rate γ_n, i.e., the fastest growing instability mode determines the splitting mode. Nevertheless, we have also seen that, in some cases, N is different from the prediction of the linear stability analysis. For example, at $s = 2$ and $\kappa = 0.13$, we have seen the splitting of the spinning soliton into *four* fragments, while the largest growth rate was found at $n = 3$ for the same values of the parameters, see figure 3b. However, as it is seen from figure 3, there is a narrow (*stability window*) for extremely broad spinning solitons.

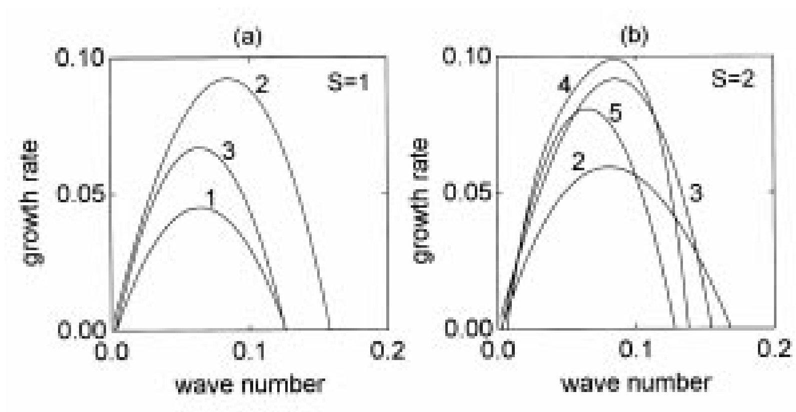

Figure 3. The growth rate of perturbation eigenmodes with different azimuthal 'quantum numbers' n vs the soliton's propagation constant κ: (**a**) $s = 1$; (**b**) $s = 2$. The labels near the curves indicate the value of n.

B. *Three-dimensional case*

In the 3D case, the underlying equation is obtained from eq. (1), replacing the transverse diffraction operator $\partial^2/\partial x^2$ by the Laplacian $\nabla_\perp^2$ acting on the transverse coordinates x and y. Accordingly, the normalized equation similar to eq. (2) takes, after the same rescalings as those which led to eq. (2), the form

$$iu_Z + u_{XX} + u_{YY} + u_{TT} + |u|^2 u - |u|^4 u = 0, \tag{11}$$

where the new coordinate y is rescaled the same way as x.

We look for stationary solutions to eq. (11) of the form $u = U(r,T)\exp(is\theta)\exp(i\kappa Z)$, where r and θ are the polar coordinates in the transverse plane, κ is a propagation constant, and the integer s is the 'spin'. The amplitude U can be taken real, and it obeys the equation (cf. eq. (3) in the 2D case)

$$U_{rr} + \frac{1}{r}U_{rr} - \frac{s^2}{r^2}U + U_{TT} - \kappa U + U^3 - U^5 = 0, \tag{12}$$

κ parametrizing the family of stationary solutions.

Equation (11) conserves energy, which in the 3D case is (cf. eq. (4))

$$E_{3D} = \int_{-\infty}^{\infty}\int_{-\infty}^{\infty}\int_{-\infty}^{\infty} |u(X,Y,T)|^2 \,\mathrm{d}X\mathrm{d}Y\mathrm{d}T, \tag{13}$$

The Hamiltonian and angular momentum in the transverse plane, which remain dynamical invariants in the 3D case, are given by expressions (cf. eqs (5) and (6))

$$H_{3D} = \int_{-\infty}^{\infty}\int_{-\infty}^{\infty}\int_{-\infty}^{\infty} \left[|u_X|^2 + |u_Y|^2 + |u_T|^2 - (1/2)|u|^4 + (1/3)|u|^6\right] \mathrm{d}X\mathrm{d}Y\mathrm{d}T, \tag{14}$$

$$L_{3D} = \int_{-\infty}^{\infty}\int_{-\infty}^{\infty}\int_{-\infty}^{\infty} (\partial\phi/\partial\theta)\,|u|^2 \mathrm{d}X\mathrm{d}Y\mathrm{d}T, \tag{15}$$

ϕ again being the phase of the complex field u.

One readily finds from eq. (12) that the values of L_{3D} and H_{3D} for the stationary spinning LBs are related to its energy as follows: $L_{3D} = sE_{3D}$, and (cf. eq. (7))

$$H_{3D} = \kappa E_{3D} - \frac{2}{3}\int_{-\infty}^{\infty}\int_{0}^{\infty} 2\pi r U^6(r,T)\mathrm{d}r\mathrm{d}T. \tag{16}$$

We have numerically found one-parameter families of the 3D spinning solitons which have the form of a doughnut with a hole in the center [32]. In accordance with the results predicted by means of the semi-analytical variational approximation developed in ref. [23], the solutions exist provided that their energy exceeds a certain threshold value. As an additional test of the accuracy of numerical computations, we have used a relation which can be obtained directly from eq. (12), cf. eq. (8):

$$\kappa E_{3D} = (1/4)\int_{-\infty}^{\infty}\int_{0}^{\infty} 2\pi r U^4 \mathrm{d}r\mathrm{d}T. \tag{17}$$

In order to quantify the 3D LB solutions, similar to the 2D case (see figure 1), we show in figure 4 the propagation constant κ and the Hamiltonian H_{3D} of the zero-spin ($s = 0$) and spinning LBs, with $s = 1$ and $s = 2$, vs. their energy E_{3D}. It is evident that, in accordance with ref. [23], the threshold energy strongly increases with the value of the spin. In figure 4, full and dashed lines correspond, respectively, to stable and unstable branches, as per direct numerical results for the stability presented below. In particular, it will be seen that only the $s = 0$ solitons may be fully stable. The $s = 0$ branch of the solutions in figure 4 is divided into stable and unstable portions on the basis of the known Vakhitov-Kolokolov criterion [39].

As concerning the radial profile of the 3D solitons, it was found that with the increase of κ, the amplitude of the solitons attains a maximum at $\kappa_{\max} \simeq 0.113$ for $s = 0$, and at $\kappa_{\max} \simeq 0.138$ for $s = 1$ and $s = 2$. For $\kappa > \kappa_{\max}$, the soliton's amplitude decreases and its shape becomes flatter. It is relevant to mention that the semianalytical approximation of ref. [23] yields very close results for the characteristics of the stationary solutions. For instance, it predicted that, for $s = 1$, the threshold energy was $E_{\text{thr}} = 750$, and this value was attained at $\kappa = 0.033$, cf. figure 4a.

Figures 5 through 7 show some representative gray-scale contour plots of the intensity $|u(X,Y,T=0)|^2$. They display the most important result: by direct numerical simulations of eq. (11), we have found that the spinning LBs are *always* unstable against azimuthal

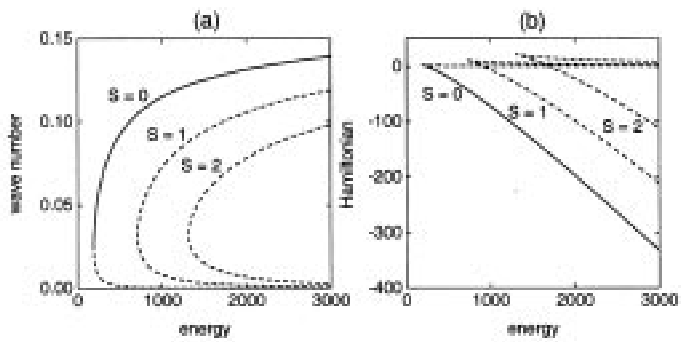

Figure 4. The propagation constant κ (**a**) and Hamiltonian H_{3D} (**b**) of the three-dimensional spinning light bullet vs. its energy E_{3D}.

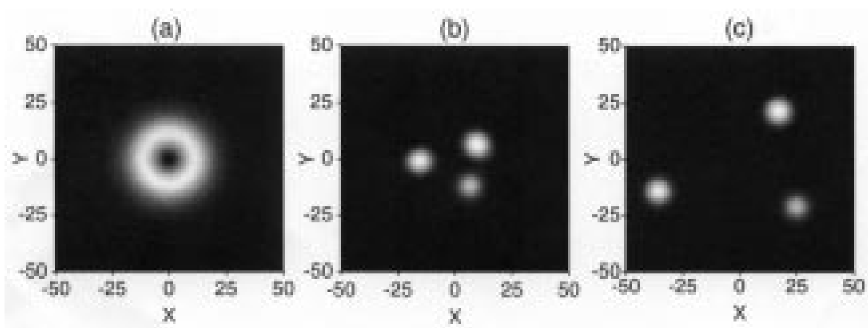

Figure 5. Gray-scale contour plots illustrating the instability of the three-dimensional spinning light bullet with $s = 1$ and $\kappa = 0.01$: (**a**) $Z = 0$, (**b**) $Z = 520$, and (**c**) $Z = 600$.

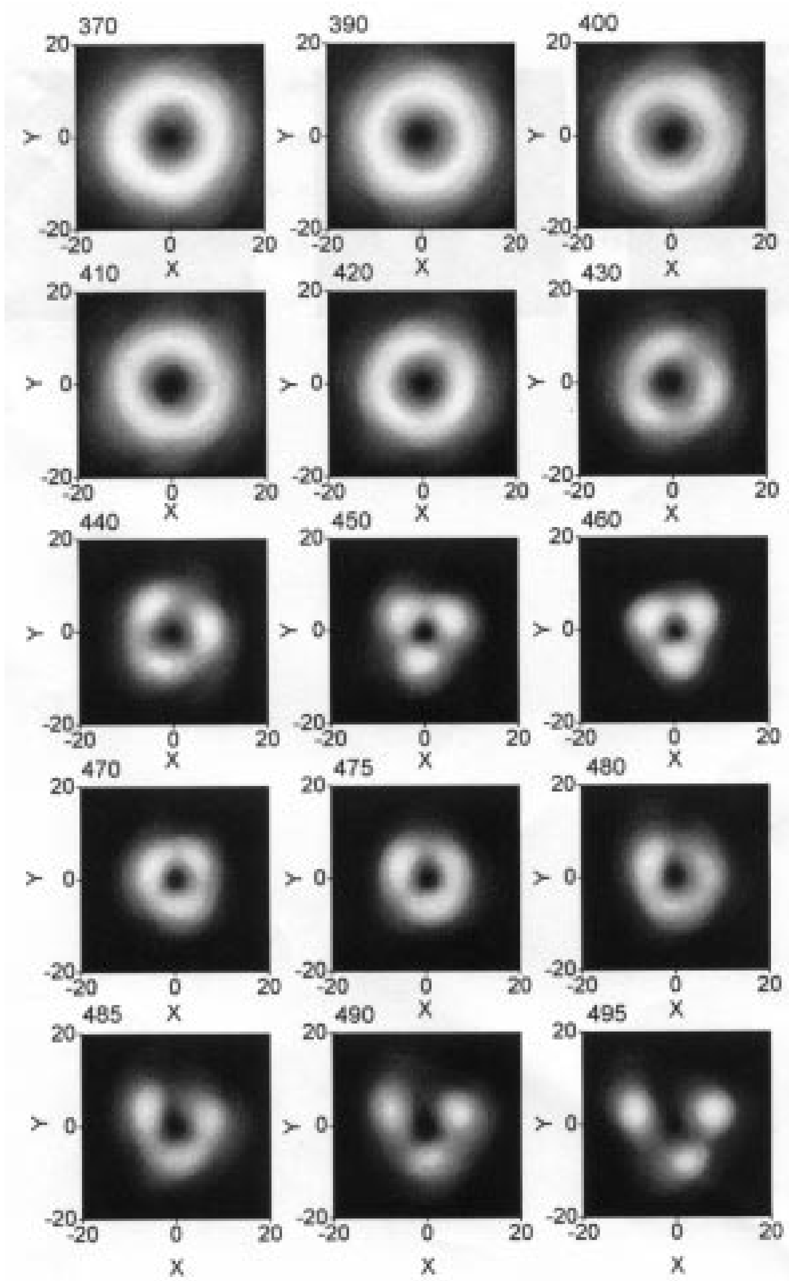

Figure 6. The pre-splitting evolution of a three-dimensional spinning light bullet with $s = 1$ and $\kappa = 0.01$.

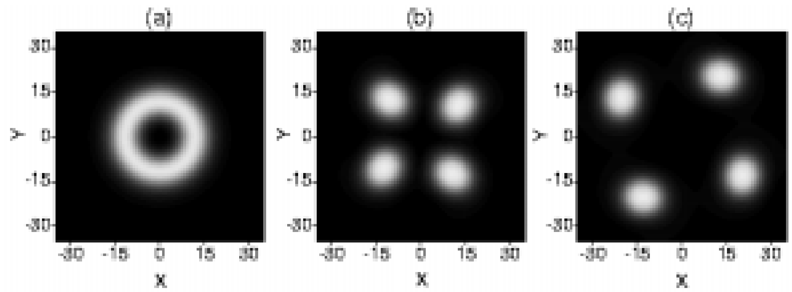

Figure 7. Grey-scale contour plots illustrating the instability of the three-dimensional light bullets with spin $s = 2$ and $\kappa = 0.08$: (**a**) $Z = 0$, (**b**) $Z = 230$, and (**c**) $Z = 260$.

perturbations. As well as in the 2D case, the instability eventually leads to a breakup of the doughnuts into several moving zero-spin solitons.

It is noteworthy that the instability mode seemingly dominating the splitting of the spinning soliton in the case shown in figure 6 may be interpreted as the one related to a spontaneous shift of the soliton's central 'bubble' (note that the corresponding unperturbed LB is not very broad). In this case, the pre-splitting evolution of the soliton is quite nontrivial: at a moderately long initial stage of the evolution, $Z < 430$ (the soliton period of the unperturbed LB is $Z_0 = 160$ in this case), it demonstrates no instability, next it develops a three-fold perturbation breaking the azimuthal symmetry, which, however, disappears, causing an appreciable shrinkage of the soliton at $Z = 475$, and finally a perturbation that may indeed be interpreted as a shift of the central bubble sets in, quickly cleaving the soliton into *three* moving nonspinning fragments.

The stability of spinning solitons against this bubble-shift mode was recently studied analytically in ref. [33]. It has been demonstrated that the 2D and 3D spinning solitons are unstable against this mode in the cases $s = 1$ and $s = 2$. Of course, the absence of the instability of LBs with $s \geq 3$ against this particular perturbation mode does not mean that they are stable, as other modes (dipole or multipole ones, as opposed to the *monopole* bubble-shift mode considered in ref. [33]) may also give rise to instability. Moreover, it may easily happen that the higher-order modes generate a stronger instability, which may explain the fact that the development of the instability through the spontaneous shift of the central bubble is not seen in other examples displayed above, viz., figures 2, 5, and 7 for the 2D and 3D spinning LBs, respectively.

Getting back to the description of general features of the spinning-soliton splitting induced by the azimuthal instability, we note that the three fragments emerging in the case of a smaller initial energy of the spinning LB (smaller κ) have *unequal energies* and, accordingly, unequal intensities at their central points (see figure 5). We have also found that, with the increase of the initial energy, the number of the fragments decreases from three to two. In the latter case, the two fragments have exactly equal energies.

For LBs with $s = 2$, we have found that a typical outcome is their splitting into four fragments with *equal energies* (see figure 7). Thus, we conclude that, as well as in the 2D case, the initial internal angular momentum of the spinning LB is converted into the orbital momentum of the emerging fragments, which fly out tangentially to the circular crest of the doughnut soliton. Running much more simulations, we have found that the number of the fragments is, roughly, twice the original spin s.

Despite the instability of the spinning LBs, they may have a chance to be observed in a finite-size bulk sample if the instability is developing slowly enough, so that the LB may survive over the propagation distance several times larger that the corresponding soliton period Z_0 (as well as in the 2D case, $Z_0 \equiv \pi/2\kappa$). To compare Z_0 and the propagation distance over which the LB survives, we notice that, in the case $s = 1$ and $\kappa = 0.01$, which corresponds to the case displayed in figure 5, numerical data show that the splitting actually commences at $Z_{\text{split}} \simeq 400$, while the corresponding soliton's period is $Z_0 \approx 160$. Thus, the obtained ratio $Z_{\text{split}}/Z_0 \approx 2.5$ is at the border of the range in which the LB can be a physically meaningful object.

However, in the case $s = 1$ and $\kappa = 0.08$, we find $Z_{\text{split}} \simeq 550$, while $Z_0 \approx 20$, so that in this case LB may be regarded as a *virtually stable* object. Generally, we observed a clear trend to the stabilization of the spinning LBs with the increase of their energy (i.e., increase of κ), the same as what was concluded above for 2D spinning solitons.

The instability turns out to be much stronger for $s = 2$: in the case $\kappa = 0.01$, we find $Z_{\text{split}} \simeq 130$, and for $\kappa = 0.08$, the result is $Z_{\text{split}} \simeq 180$. Thus, it would be less feasible, but not impossible, to experimentally observe LBs with $s = 2$. Probably, there is no chance to observe those with $s > 2$.

3. Spinning solitons in dissipative cubic-quintic nonlinear media

Complex Ginzburg-Landau equations constitute a class of universal models describing pattern formation in a great variety of nonlinear dissipative systems [40]. Among the patterns, localized pulses are especially interesting. While the theory of pulses in various 1D models of the GL type was well elaborated [40–43], much less is known about 2D localized patterns (2D pulses).

In order to make the pulses stable, it is first of all necessary to stabilize its zero background (trivial solution to the GL equation), which can be done within the framework of the CQ GL equation [7–12,41], or a model linearly coupling a cubic GL equation to a linear dissipative one [10]. Although the CQ GL equation was originally introduced by Sergeev and Petviashvili [41] in a 2D form, exactly in order to generate 2D localized pulses in the form of 'spiral solitons', much more work has been done to investigate not 'solitons' of this type, but rather spiral waves extending to infinity [44,45]. In particular, the stability of delocalized spiral vortices in a model of a superflow, and interactions of vortices in a two-component GL system have been investigated in refs [46] and [47]. On the other hand, nonspiraling axisymmetric 2D patterns in the form of localized 'bubbles' were recently studied in other models, e.g., the complex Swift-Hohenberg equation [48].

An analysis of *spiral solitons* of the complex CQ GL equation, i.e., localized 2D objects with an internal vorticity, which, as well as the vortex-ring solitons in conservative models, are characterized by an integer-valued 'spin' s, was recentlty performed in ref. [49]. As well as in the conservative case, a crucially important issue is the soliton's stability at different values of s.

Note that, in the dissipationless limit, the GL equation goes over into an equation of the NLS type. Accordingly, a spiral soliton turns into a 2D spinning soliton of the type considered above. However, a principal difference is that that the GL equation may only have a few isolated solitary-pulse solutions (normally, two, if one of them is expected to be stable, the second pulse playing the role of an unstable *separatrix* [10]), while its NLS counterpart, as it was demsonstrated above, has a continuous family of soliton solutions which may be parametrized by their energy. In the case when all the dissipative parameters of the GL model are small, i.e., it may be considered as a perturbation of its NLS counterpart, isolated pulses that survive as solutions to the GL equation are selected from the continuous family of the NLS solitons by a condition of balance between gain and losses [10].

One may expect that, on the contrary to the conservative NLS equation, in the GL model the vortex ring may be *stable*. Indeed, in the limit when the external size of the ring diverges, the vortex ring turns into a usual delocalized rotating spiral wave [45]. It is known that, generally, the latter wave in dissipative systems has a finite (nonzero) *stability margin* against the spontaneous off-center shift of its inner bubble. On the other hand, in the same limit, the vortex ring in the NLS equation turns into a usual delocalized 'optical vortex' (2D dark soliton) [50], which is, obviously, only *neutrally stable* against the spontaneous shift of the inner bubble. Therefore, the interaction of the inner bubble with the outer rim of the large-size but finite NLS soliton may destabilize the whole ring, turning the neutral shift mode into an unstable one, which, as it was explained above, is indeed the case in the CQ NLS equation [33]; however, the above-mentioned stability margin of the inner bubble against the shift inside the GL spiral wave may help to stabilize a *finite-size* spiral soliton too in the GL equation. Our simulations will show that it is indeed relatively easy to find a spiral soliton which is fairly stable against all the perturbations, including azimuthal ones which are fatal for the NLS vortex ring.

We consider the (2+1)-dimensional CQ complex GL equation in a general form,

$$iA_z + i\delta \cdot A + (1/2 - i\beta)(A_{xx} + A_{yy}) + (1 - i\varepsilon)|A|^2 A - (\nu - i\mu)|A|^4 A = 0. \tag{18}$$

The equation is written in the 'optical' notation, assuming evolution along the propagation coordinate z of a beam with the 2D cross section in the plane (x,y). In fact, bulk (3D) optical media is the most appropriate system for experimental generation of vortex rings, see, e.g., ref. [26]. In that case, $A(x,y;z)$ is the local amplitude of the electromagnetic wave, the diffraction and cubic-self-focusing coefficients are normalized to be 1, ε is the cubic gain, δ and μ are the linear and quintic loss parameters (as a matter of fact, the latter one accounts for the nonlinear gain saturation in optical media), and ν is the quintic self-defocusing coefficient. Lastly, β is an effective diffusion coefficient (in optical media, diffusion takes place if light creates free charge carriers, which may take place, e.g., in semiconductor waveguides).

The spiral solitons are axisymmetric solutions to eq. (18) of the form $A(x,y;z) = U(z,r)\exp(is\theta)$, where r and θ are polar coordinates in the (x,y) plane, and s is the above-mentioned integer 'spin' (topological charge of the vortex). The complex amplitude $U(z,r)$ obeys an equation

$$\begin{aligned} &iU_z + i\delta \cdot U + (1/2 - i\beta)(U_{rr} + r^{-1}U_r - s^2 r^{-2} U) + (1 - i\varepsilon)|U|^2 U \\ &\quad -(\nu - i\mu)|U|^4 U = 0, \end{aligned} \tag{19}$$

which is supplemented by boundary conditions stating that $U \sim r^s$ at $r \to 0$, and $U(r)$ decays exponentially at $r \to \infty$. Note that the localized solution can be interpreted as a *spiral soliton* because the function $U(r)$ is complex, $U(r) \equiv |U(r)| \exp(i\Phi(r))$, hence equal-phase curves $s\theta + \Phi(r) = \text{const}$ are spirals, rather than straight lines $s\theta = \text{const}$, as in the case of the CQ NLS equation, where $U(r)$ is real [31,23].

The first purpose is to find stationary localized solutions to eq. (19) which must be stable within the framework of this equation, i.e., they must be *attractors*, similarly to stable solitons in various forms of the 1D GL equation [8–12]. As the stability of the spiral solitons against the most dangerous azimuthal perturbations is not comprised by eq. (19), it will be considered below separately.

In order to find the solutions, we have performed numerical simulations of eq. (19) at many different values of parameters and using various initial configurations $U(r;z=0)$. Typical examples of the formation of spiral solitons with spin $s=1$ and $s=2$ are shown in figure 8. In particular, in the case $s=2$, this resembles the formation of a 'composite pulse', which was found to be stable in the 1D GL model studied in ref. [12]. However, a direct analog of the 'composite pulse' in the present (2+1)D model has never been found. The spinning solitons, as well as the nonspinning ones, are found to be strong attractors, as they can be generated from a large variety of inputs. Another important finding is that stable solitons with different values of the vorticity considered here, $s = 0,1,2$, *coexist* in a large domain of the parameter space, see details below (we will also display a smaller region of the parameter space, in which stable solitons with $s=1$ and $s=2$ coexist, while zero-spin solitons were not found). In other words, each soliton is a strong attractor inside its own class of pulses, distinguished by the value of the spin, which plays the role of a *topological invariant*.

An important characteristic of solitons is their *integral power* (which is sometimes also called 'energy', or 'intensity'). It is defined in the usual way, as $I = 2\pi\int_0^{+\infty} |U(r)|^2\, r\mathrm{d}r$. The power has been found to take very different values for the coexisting solitons with different values of the spin. This is illustrated by figure 9a, where the power is shown as a function of the nonlinear quintic loss parameter μ.

To proceed from the typical examples displayed above to the presentation of systematic results, in figure 9b we display the existence domains for both spinning and nonspinning solitons in the parameter plane (ε,μ). In the black region, there exist both spinning and nonspinning stable solitons, whereas in the lower white strip *only spinning* solitons have been found to form. In the gray region, solitons do not form at all. Lastly, in the upper white region, initial pulses have been found to expand indefinitely, generating an advancing front similar to a 1D structure investigated in detail in ref. [12].

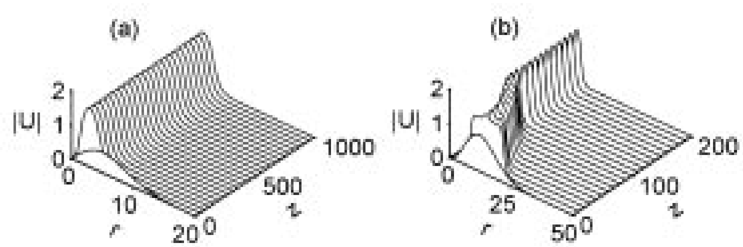

Figure 8. Formation of two-dimensional spinning solitons from the Gaussian initial field configurations: (**a**) $s=1$ and (**b**) $s=2$. The parameters are: $\beta = 0.5$, $\delta = 0.5$, $\nu = 0.1$, $\mu = 1$ and $\varepsilon = 2.5$. The initial field distributions are: (**a**) $U(r;z=0) = 0.2\, r\exp[-(r/7)^2]$, and (**b**) $U(r;z=0) = 0.02\, r^2\exp[-(r/12)^2]$.

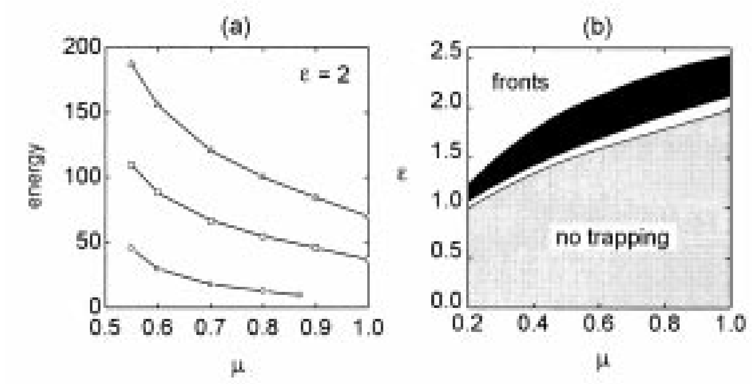

Figure 9. (**a**) The integral power I versus quintic loss μ for a fixed cubic gain $\varepsilon = 2$. The other parameters are $\beta = 0.5$, $\delta = 0.5$ and $\nu = 0.1$. The circles, squares, and triangles correspond to, respectively, nonspinning solitons, spinning solitons with $s = 1$, and spinning solitons with $s = 2$. (**b**) The existence domain in the parameter plane (ε, μ) for both spinning and nonspinning stable solitons. The other parameters are $\beta = 0.5$, $\delta = 0.5$ and $\nu = 0.1$.

In other regions of the parameter space we have found apparently stable nonspinning and spinning pulsating solutions (*breathers*), which demonstrate persistent quasiperiodic internal vibrations, similar to those found in the 1D version of CQ GL equation [11,12]. These robust pulsating solitons are a characteristic feature of dissipative physical systems and they do not have anything in common with the superposition of zero-velocity solitons of the NLS equation which produces pulsating solutions. We mention also that the nonspiraling ($s = 0$) and spiraling ($s = 1, 2$) breathers coexist with each other at the same values of the parameters, whereas the stationary (nonvibrating) solitons do *not* exist at these parameter values.

As it was explained above, the comparison with the spinning solitons in the CQ NLS model strongly suggests that the overall stability of the solitons is determined by azimuthal perturbations breaking the axial symmetry of the solutions. Recall that the above equation (19) cannot include azimuthal perturbations. Therefore, in order to test this kind of the stability, we have simulated the full equation (18) directly in the Cartesian coordinates. Doing this, we have found that both nonspinning and spiral solitons found above from eq. (19) are remarkably *stable* against azimuthal perturbations, in accordance with the qualitative arguments presented before.

Although large-scale simulations of the full underlying equation are quite sufficient to predict observation of stable solitons in experiments, this does not provide for a mathematically complete evidence of the solitons' stability. As well as in the case of the solitons in conservative media, a direct way to prove the true stability is to consider the eigenvalue problem produced by the linearization of the evolution equation around the corresponding stationary solutions. We have performed this analysis too, aiming to compute the largest growth rates (eigenvalues) of the azimuthal perturbation eigenmodes for different values of the perturbation index n, which is defined in the same way as in eq. (9) for the case of the spinning solitons in conservative media. In *all the cases* when the direct simulations produced apparently stable stationary solitons, we have found that the largest growth rate of the perturbation eigenmodes has a *negative* real part, thus corroborating the stability of the corresponding stationary solitons.

In order to assess the range in the space of the initial configurations for which the stable solitons are attractors, we have additionally performed a large number of direct simulations with initial pulses in the form of Gaussians with intrinsic vorticity. Simulations of this kind are necessary because, in a real experiment, input pulses normally have the Gaussian shape (the vorticity can easily be lent to a pulse by passing it through a phase mask [26]). In all the cases in which the existence of stable spiral solitons was known, the initial Gaussians rapidly developed into them, keeping the initial value of the spin. To illustrate this, in figures 10a and 10b we display gray-scale plots representing the amplitude and phase of the initial Gaussian beam, which was taken as

$$A(x,y;z=0) = 1.6\exp\left[-(x^2+y^2)/25\right]\cdot\exp(i\theta),$$

whereas in figures 10c and 10d the amplitude and phase of the established doughnut-shaped soliton are shown at $z=150$.

Lastly, we note that the phase plot corresponding to the established soliton displayed in figure 10d clearly shows a spiral structure, justifying the application of the term 'spiral solitons' to the 2D solitary-wave patterns considered in this work.

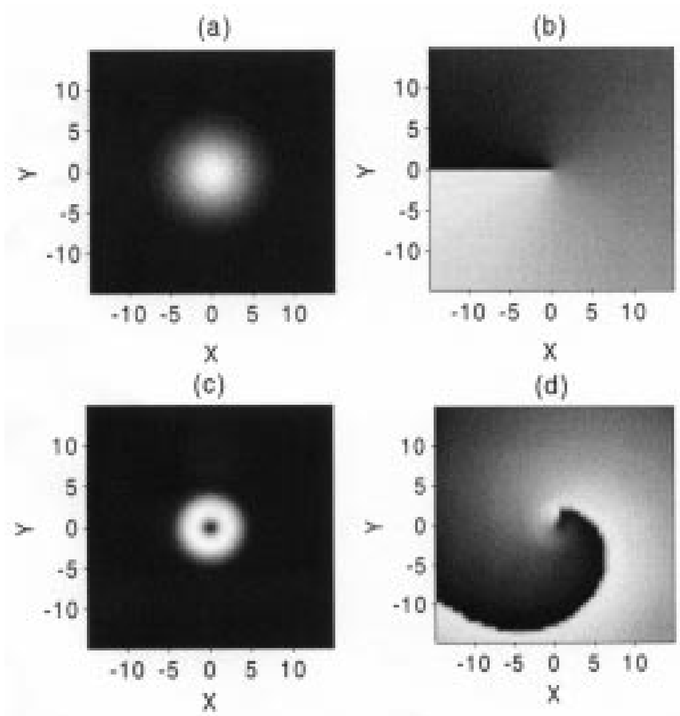

Figure 10. Gray-scale plots of the input Gaussian field with the vorticity $s=1$: (**a**) amplitude and (**b**) phase. The output field at $z=150$: (**c**) amplitude and (**d**) phase. The parameters are $\beta=0.5$, $\delta=0.5$, $\nu=0.1$, $\mu=1$ and $\varepsilon=2.5$.

A challenging problem is the interaction between spiral solitons with equal or different vorticities (interactions between spirals extending to infinity have been already studied in detail by means of analytical and numerical methods [45]). If the solitons are far separated, and their vorticities are equal or opposite, the interaction can be described analytically in terms of an effective potential, using a technique elaborated in ref. [51]. However, in the most interesting case when the solitons are essentially overlapped and, hence, they interact strongly, heavy direct simulations are necessary.

4. Conclusions

In this paper, we have presented a survey of recent results concerning the existence and stability of nonspining and, chiefly, spinning solitons in both nonlinear Schrödinger and Ginzburg-Landau (i.e., conservative and dissipative) complex equations combining cubic and quintic nonlinearities. In the former case, both two- and three-dimensional solitons have been considered. In the latter case, the (two-dimensional) spinning soliton actually has a form of a localized spiral wave.

The main qualitative inference is that the spinning solitons of relatively low energy in the conservative model are always subject to an instability breaking their axial symmetry and leading to splitting of the soliton into several fragments flying out in tangential directions, each one being a (perfectly stable) zero-spin soliton. Contrary to this, the spiral solitons in the two-dimensional cubic-quintic Ginzburg-Landau equation may be fully stable, and they may coexist at different values of the spin. Moreover, the two-dimensional cubic-quintic Ginzburg-Landau equation also gives rise to stable nonspinning and spiral pulsating solitons (breathers), which coexist with each other, but do not coexist with the nonvibrating solitons.

Acknowledgments

We appreciate valuable discussions with N N Akhmediev, A V Buryak, F Lederer, D Neshev, L M Pismen, and J M Soto-Crespo.

References

[1] A C Newell, *Solitons in mathematics and physics* (Society for Industrial and Applied Mathematics, Philadelphia, 1985)

[2] N N Akhmediev and A Ankiewicz, *Solitons: Nonlinear Pulses and Beams* (Chapman and Hall, London, 1997)

[3] H A Haus, J G Fujimoto and E P Ippen, *J. Opt. Soc. Am.* **B8**, 2068 (1991)
P K Jakobsen, J V Moloney, A C Newell and R Indik, *Phys. Rev.* **A45**, 8129 (1992)
J D Moores, *Opt. Commun.* **96**, 65 (1993)

[4] L M Hocking and K Stewartson, *Proc. R. Soc. London* **A326**, 289 (1972)
P Kolodner, *Phys. Rev.* **A44**, 6466 (1991)

[5] P A Bélanger, L Gagnon, and C Paré, *Opt. Lett.* **14**, 043 (1989)
G P Agrawal, *Phys. Rev.* **A44**, 7493 (1991)
B A Malomed, M Gölles, I M Uzunov and F Lederer, *Phys. Scr.* **55**, 73 (1997)

B A Malomed, A G Vladimirov, G V Khodova and N N Rosanov, *Phys. Lett.* **A274**, 111 (2000)
[6] N R Pereira and L Stenflo, *Phys. Fluids* **20**, 1733 (1977)
K Nozaki and N Bekki, *J Phys. Soc. Jpn.* **53**, 1581 (1984)
R Conte and M Musette, *Physica* **D69**, 1 (1993)
D Anderson, F Cattani and M Lisak, *Phys. Scr.* **T82**, 32 (1999)
[7] B A Malomed, *Physica* **D29**, 155 (1987) (see Appendix in this paper)
O Thual and S Fauve, *J. Phys. (Paris)* **49**, 1829 (1988)
S Fauve and O Thual, *Phys. Rev. Lett.* **64**, 282 (1990)
[8] W van Saarloos and P Hohenberg, *Phys. Rev. Lett.* **64**, 749 (1990)
V Hakim, P Jakobsen and Y Pomeau, *Europhys. Lett.* **11**, 19 (1990)
B A Malomed and A A Nepomnyashchy, *Phys. Rev.* **A42**, 6009 (1990)
[9] N Akhmediev and V V Afanasjev, *Phys. Rev. Lett.* **75**, 2320 (1995)
[10] B A Malomed and H G Winful, *Phys. Rev.* **E53**, 5365 (1996)
J Atai and B A Malomed, *Phys. Rev.* **E54**, 4371 (1996); *Phys. Lett.* **A246**, 412 (1998)
[11] H R Brand and R J Deissler, *Phys. Rev. Lett.* **63**, 2801 (1989)
R J Deissler and H R Brand, *Phys. Rev. Lett.* **72**, 478 (1994); **74**, 4847 (1995); **81**, 3856 (1998)
H Sakaguchi and B A Malomed, *Physica* **D147**, 273 (2000)
[12] V V Afanasjev, N Akhmediev and J M Soto-Crespo, *Phys. Rev.* **E53**, 1931 (1996)
J M Soto-Crespo, N Akhmediev and A Ankiewicz, *Phys. Rev. Lett.* **85**, 2937 (2000)
[13] Y Silberberg, *Opt. Lett.* **15**, 1282 (1990)
[14] J T Manassah, P L Baldeck and R R Alfano, *Opt. Lett.* **13**, 1090 (1988)
[15] A B Blagoeva, S G Dinev, A A Dreischuh and A Naidenov, *IEEE J. Quantum Electron.* **QE-27**, 2060 (1991)
[16] L Bergé, *Phys. Rep.* **303**, 260 (1998)
L Bergé, V K Mezentsev, J J Rasmussen and J Wyller, *Phys. Rev.* **A52**, R52 (1995)
L Bergé, O Bang, J J Rasmussen and V K Mezentsev, *Phys. Rev.* **E55**, 3555 (1997)
[17] R H Enns, D E Edmundson, S S Rangnekar and A E Kaplan, *Opt. Quantum Electron.* **24**, S1295 (1992)
D E Edmundson and R H Enns, *Phys. Rev.* **A51**, 2491 (1995)
[18] R McLeod, K Wagner and S Blair, *Phys. Rev.* **A52**, 3254 (1995)
[19] A A Kanashov and A M Rubenchik, *Physica* **D4**, 122 (1981)
[20] K Hayata and M Koshiba, *Phys. Rev. Lett.* **71**, 3275 (1993)
B A Malomed, P Drummond, H He, A Berntson, D Anderson and M Lisak, *Phys. Rev.* **E56**, 4725 (1997)
D V Skryabin and W J Firth, *Opt. Commun.* **148**, 79 (1998)
D Mihalache, D Mazilu, B A Malomed and L Torner, *Opt. Commun.* **152**, 365 (1998); **169**, 341 (1999)
D Mihalache, D Mazilu, J Dörring and L Torner, *Opt. Commun.* **159**, 129 (1999)
[21] D Mihalache, D Mazilu, L-C Crasovan, L Torner, B A Malomed, and F Lederer, *Phys. Rev.* **E62**, 7340 (2000) (1 November issue)
[22] M Quiroga-Teixeiro, A Berntson and H Michinel, *J. Opt. Soc. Am.* **B16**, 1697 (1999)
[23] A Desyatnikov, A Maimistov and B Malomed, *Phys. Rev.* **E61**, 3107 (2000)
[24] X Liu, L J Qian and F W Wise, *Phys. Rev. Lett.* **82**, 4631 (1999)
X Liu, K Beckwitt and F W Wise, *Phys. Rev.* **E61**, R4722 (2000); **62**, 1328 (2000)
[25] L Torner and D V Petrov, *Electron. Lett.* **33**, 608 (1997)
D V Petrov and L Torner, *Opt. Quantum Electron* **29**, 1037 (1997)
W J Firth and D V Skryabin, *Phys. Rev. Lett.* **79**, 2450 (1997)
D V Skryabin and W J Firth, *Phys. Rev.* **E58**, 3916 (1998)
[26] D V Petrov, L Torner, J Martorell, R Vilaseca, J P Torres and C Cojocaru, *Opt. Lett.* **23**, 1444 (1998)

[27] D Mihalache, D Mazilu, L-C Crasovan, B A Malomed and F Lederer, *Phys. Rev.* **E62**, R1505 (2000)
[28] A V Buryak and Y S Kivshar, *Phys. Rev.* **A51**, R41 (1995)
S Trillo and P Ferro, *Opt. Lett.* **20**, 438 (1995)
P Drummond, H He and B A Malomed, *Opt. Commun.* **123**, 394 (1996)
[29] P Di Trapani, W Chinaglia, S Minardi, A Piskarskas and G Valiulis, *Phys. Rev. Lett.* **84**, 3843 (2000)
[30] E W Wright, B L Lawrence, W Torruellas and G I Stegeman, *Opt. Lett.* **20**, 2481 (1995)
B. L Lawrence and G I Stegeman, *Opt. Lett.* **23**, 591 (1998)
[31] M Quiroga-Teixeiro and H Michinel, *J. Opt. Soc. Am.* **B14**, 2004 (1997)
[32] D Mihalache, D Mazilu, L-C Crasovan, B A Malomed and F Lederer, *Phys. Rev.* **E61**, 7142 (2000)
[33] B A Malomed, L-C Crasovan and D Mihalache, *Physica* **D** (to be published)
[34] D Neshev, private communication
[35] A G Truscott, M E J Friese, N R Heckenberg and H Rubinsztein-Dunlop, *Phys. Rev. Lett.* **82**, 1438 (1999)
[36] Z H Musslimani, M Segev, D N Christodoulides and M Soljaćić, *Phys. Rev. Lett.* **84**, 1164 (2000)
[37] N N Akhmediev, V I Korneev and Yu V Kuz'menko, *Zh. Eksp. Teor. Fiz.* **88**, 107 (1985) [*Sov. Phys. JETP* **61**, 62 (1985)]
J M Soto-Crespo, D R Heatley, E M Wright and N N Akhmediev, *Phys. Rev.* **A44**, 636 (1991)
J Atai, Y Chen and J M Soto-Crespo, *Phys Rev.* **A49**, R3170 (1994)
[38] D E Edmundson, *Phys. Rev.* **E55**, 7636 (1997)
[39] M G Vakhitov and A A Kolokolov, *Izv. Vuz. Radiofiz.* **16**, 1020 (1973) [*Sov. J. Radiophys. Quantum Electr.* **16**, 783 (1973)]
[40] M C Cross and P C Hohenberg, *Rev. Mod. Phys.* **65**, 851 (1993)
[41] A M Sergeev and V I Petviashvili, *Dokl. AN SSSR* **276**, 1380 (1984) [*Sov. Phys. Doklady* **29**, 493 (1984)]
[42] L Torner, J Dörring and J P Torres, *IEEE J. Quantum Electron.* **QE-35**, 1344 (1999)
[43] L-C Crasovan, B Malomed, D Mihalache and F Lederer, *Phys. Rev.* **E59**, 7173 (1999)
L-C Crasovan, B A Malomed, D Mihalache, D Mazilu and F Lederer, *Phys. Rev.* **E62**, 1322 (2000)
[44] P Coullet, L Gil and D Repaux, *Phys. Rev. Lett.* **62**, 2957 (1989)
[45] L M Pismen *Vortices in nonlinear fields* (Oxford University Press, Oxford, 1999)
[46] I Aranson and V Steinberg, *Phys. Rev.* **B53**, 75 (1996)
[47] I S Aranson and L M Pismen, *Phys. Rev. Lett.* **84**, 634 (2000)
[48] V B Taranenko, K Staliunas and C O Weiss, *Phys. Rev. Lett.* **81**, 2236 (1998)
V J Sanchez-Morcillo and K Staliunas, *Phys. Rev.* **E60**, 6153 (1999)
[49] L-C Crasovan, B A Malomed and D Mihalache, *Phys. Rev.* **E63**, 016605 (2001) (1 January issue)
[50] C T Law and G A Swartzlander, *Opt. Lett.* **18**, 586 (1993)
[51] B A Malomed, *Phys. Rev.* **E58**, 7928 (1998)